Model Experiment and Field Observation of a Snow Avalanche Deflector

Kazunori Fujisawa, *Public Works Research Institute, Ministry of Construction, Japan*

A study of the jumping-up phenomenon that occurs when a snow avalanche strikes an inclined plane was carried out. The study is important to the design of avalanche deflectors and arrestors. The behavior of an avalanche colliding with a deflector was recorded at 4-sec intervals in the field, and jumping height and length were analyzed. The results of the analysis suggest that jumping-up velocity (V_a) is less than striking velocity (V_b) against a deflector. The velocity reduction coefficient (k) is defined as V_a/V_b, and physical significance is also considered. A model experiment, in which a snow avalanche struck an inclined plane, was examined to clarify the relationship between the velocity reduction coefficient (k) and the angle of incidence (ϕ). Jumping-up height and length of the full-scale avalanche that struck the deflector were explained by using the velocity reduction coefficient (k).

A deflector is a snow avalanche protection measure constructed to control moving avalanches to protect roads and the like from damage. It is assumed that snow avalanches jump upward when they strike deflectors, so it is possible to deflect an avalanche with a structure that is taller than the jumping height. For this reason, research to clarify the behavior of a snow avalanche striking a deflector will provide information of great value in the planning and design of deflectors.

Case Study

A hamlet stands in the foothills of Mt. Gongendake in Maseguchi in the community of Nou in Niigata Prefecture, Japan. On January 26, 1986, the hamlet was devastated by a surface-layer avalanche descending from the slope of Mt. Gongendake. Disaster protection facilities constructed to protect the village from future snow avalanches include deflectors at three sites located short distances from the slope. The Niigata Prefecture Erosion Control Section used a videotape system to observe snow avalanches occurring on the slope of Mt. Gongendake, and on February 26, 1992, it obtained a video record of a snow avalanche striking Deflector 1, the deflector installed closest to the slope.

The snow avalanche is clearly observed from 15:28:56, but it is impossible to clearly observe the jumping of the avalanche after 15:30:04. Because the video images were taken at 4-sec intervals, this period was covered by 18 frames. This snow avalanche is assumed to have been a surface-layer avalanche because the pictures obtained during and immediately before the avalanche do not show any accumulated snow sliding down the slope of Mt. Gongendake. It was a relatively large-scale and flowing avalanche, and weather information from a nearby meteorological observation station indicated that the temperature on the slope where the avalanche occurred was low up to that day.

Figure 1 is a time series display made by copying the boundary conditions of the avalanche from the video images. Because the avalanche furrow topography and the steep cliffs can be confirmed (in black, Figure 1) with reference to their locations, a time series display on a plane diagram of the location of the tip of the avalanche until it struck the deflector and of the boundary shape of the avalanche afterwards can be created (Figure 2). Because

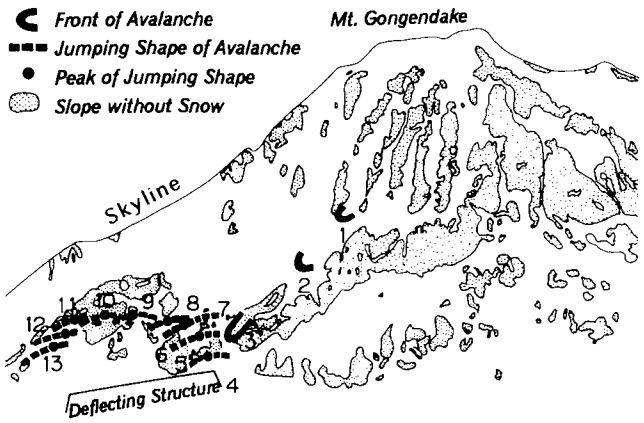

FIGURE 1 Time series diagram of snow avalanche behavior. Numbers indicate location of avalanche at 4-sec intervals.

the snow avalanche striking the deflector probably jumped in the length direction of the deflector along the deflector surface, the apparent jumping height of the avalanche can, with reference to the value of G in Figure 3, be found geometrically assuming that $H' = G + [C - (*)]$. $(*)$ is the altitude at the location of ○4, which is shown in Figure 2 and Table 1. To obtain the actual avalanche jumping height, it is necessary to deduct the snow depth from the apparent values obtained. The maximum apparent values from each frame were organized as H' in Table 1, and the locations

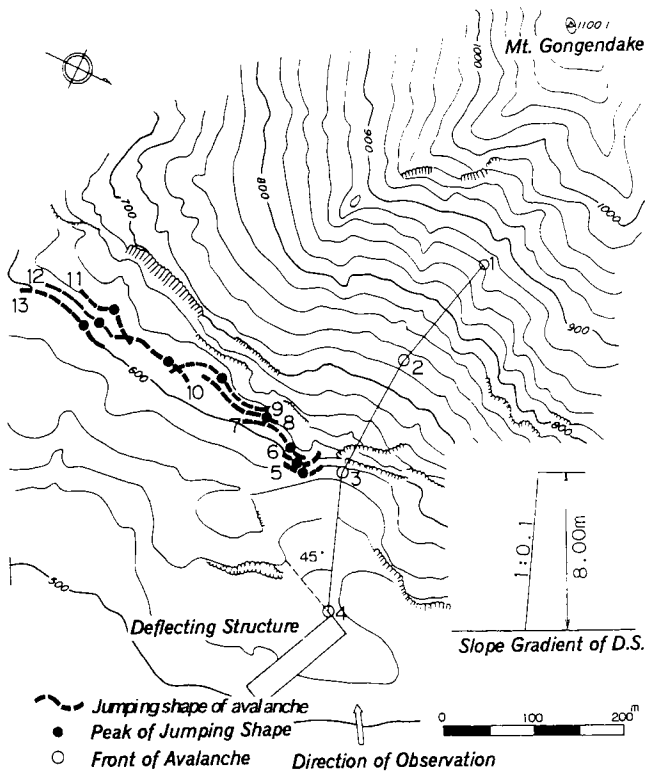

FIGURE 2 Plane diagram based on Figure 1.

at which they occurred are marked in Figure 1 and Figure 2 with black circles.

The maximum value of the apparent snow avalanche jumping height H' shown in Table 1 is 34 m, but because the interval between the images was 4 sec, it is assumed that the maximum value of H' is a little higher than 34 m. Although the accumulated snow depth around the deflector was not measured, the depth of the snow was probably very deep—probably greater than 2 m—because the depth of the snow around the spot where the video camera was installed was 2 m, and debris produced by snow avalanches descending from the slope of Mt. Gongendake was observed to pile up in front of the deflector, as it did every year. For these reasons, an estimate of the jumping height of an actual snow avalanche of about 30 m probably is close to the truth.

Study of Energy Dissipation Mechanism

The resistance to a snow avalanche is assumed to be the resistance generated by boundary friction and the resistance generated by internal friction. The resistance caused by the internal friction is assumed to consist of the resistance caused by contact between snow ice particles, the resistance produced by the turbulence of the air between the snow ice particles, and the resistance generated by the nonelastic collisions of snow ice particles. According to the particle flow resistance model (*1*), it is possible to represent the resistance stress caused by the internal friction (τ) as follows by using the contact resistance stress of the particles (τ_y), the turbulence resistance stress of the air (τ_f), and the impact resistance stress between the particles (τ_g).

$$\tau = \tau_y + \tau_f + \tau_g$$

$$\tau_y = \sigma_m \times \mu_k$$

$$\tau_f = \eta\left(\frac{du}{dy}\right) + \rho\ell^2\left|\frac{du}{dy}\right|\left(\frac{du}{dy}\right)$$

$$\tau_g = \left(\frac{\pi}{12}\right)\sin^2\alpha\left(1-e^2\right)\sigma\left(\frac{1}{b}\right)D^2\left(\frac{du}{dy}\right)^2$$

where

σ_m = vertical effective stress,
μ_k = kinematics friction coefficient,
η = coefficient of viscosity of the air,
ρ = density of the air,
ℓ = mixture length of the air based on the Prandtl,
du/dy = velocity gradient between particle rows,
α = striking angle of the particles,
e = reaction coefficient of the particles,
σ = concentration of the particles,
b = coefficient stipulating the particle interval, and
D = diameter of the particles.

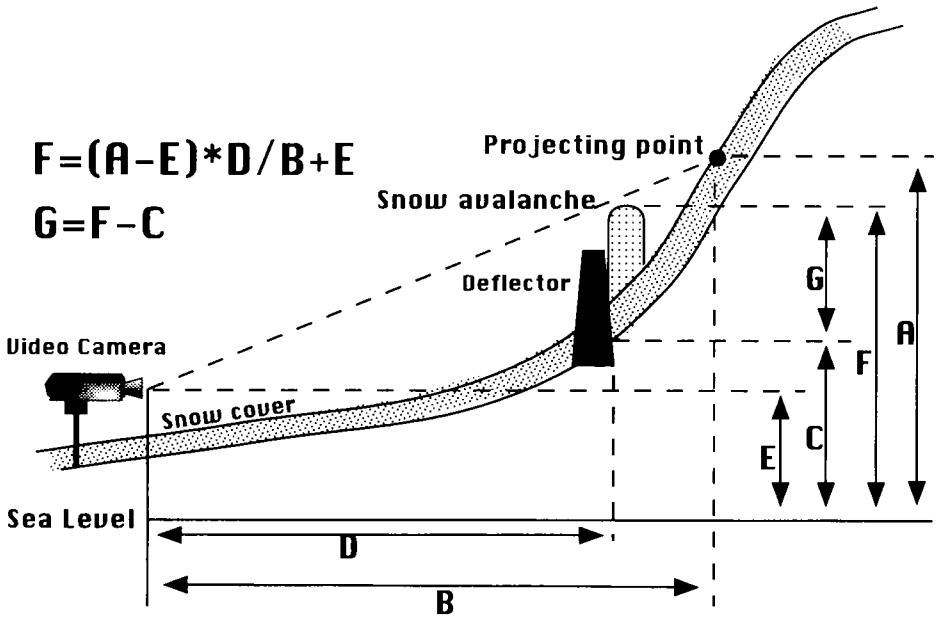

FIGURE 3 Geometric calculation for avalanche jumping height.

TABLE 1 Geometric Analysis of Avalanche Jumping Phenomenon in Collision with Deflector 1

No.	Time	A(m)	B(m)	C(m)	D(m)	E(m)	F(m)	G(m)	A.J.H. H'(m)	H.D. (m)	J.L. L(m)
1	15:28:56	B.C	B.C.	B.C.	B.C.	281	B.C.	B.C.	B.C.		B.C.
2	15:29:00					281				138(35)	
3	15:29:04					281				134(34)	
4	15:29:08	U.K.	U.K.	530 (*)	1238	281	U.K.	U.K.	U.K.	166(42)	U.K.
5	15:29:12	580	1396	530	1236	281	546	16	16	7	7
6	15:29:16	590	1406	530	1234	281	552	22	22	5	12
7	15:29:20	600	1426	530	1232	281	557	27	27	5	17
8	15:29:24	620	1460	530	1220	281	564	34	34	21	38
9	15:29:28	630	1510	518	1202	281	559	41	29	39	77
10	15:29:32	630	1540	507	1180	281	548	41	18	46	123
11	15:29:36	620	1610	494	1160	281	525	31	- 5	37	160
12	15:29:40	610	1600	480	1156	281	519	39	- 11	16	176
13	15:29:44	610	1600	474	1152	281	518	44	- 12	14	190

A.J.H.; Appeared Jumping Heights
H.D. ; Horizontal Distances
J.L. ; Jumping Lengths

B.C. ; Before Collision
U.K. ; Unknown

In the case of a snow avalanche that strikes a snow avalanche deflector, when the direction of the motion of a snow avalanche changes, the effect of inertial force is added to τ_y. It is forecast that at the same time as the turbulence of the flow increases and the mixture distance of the air increases, both the striking velocity between the particles, which governs τ_g, and the striking frequency rise. Because this means that the resistance of τ_y, τ_f, and τ_g increases, the velocity of the avalanche after it strikes the deflector is less than its striking velocity. If the striking velocity is V_b and the velocity after striking is V_a, then $V_a/V_b = k$ is defined as the velocity reduction coefficient. The value of k plays an important role in governing the jumping of an avalanche. But as this study has revealed, because the velocity reduction caused by the striking occurs during a period from the beginning of the impact at the particle level to the point where the direction of the motion has completely changed, the values of V_a and k are not defined at the striking point. Finding this value of k analytically is difficult, so it is estimated from snow ice particle striking experiments.

Study of Motion of Mass Points Striking a Plane

As shown in Figure 4, four angles based on the collision of mass points with a plane are defined. Considering the motion of an avalanche striking the deflector surface (Surface B) in the direction from I to O along the plane of incidence of the snow avalanche (Surface A), the angle of incidence of the snow avalanche that strikes Surface B (ϕ) and the run-up angle to Surface B (ψ) can be represented by using θ and β.

$$\phi = \sin^{-1}(\sin\theta \cdot \sin\beta) \tag{1}$$

$$\psi = \cos^{-1}\frac{\cos\theta}{\cos\left[\sin^{-1}(\sin\theta \cdot \sin\beta)\right]} \tag{2}$$

If the vertical Surface C is introduced to Surface B, which includes the incidence line, and the position of IV is set such that $\angle$ I,IV,O = 90°, the straight line I,IV is the normal line of Surface B and $\angle$ I,IV,III = 90° is established at the same time. And if the position of III is set such that $\angle$ O,III,IV = 90°, the straight line O,III is the normal line of the plane I,III,IV, and $\angle$ O,III,I = 90° is established at the same time. It is possible for this formula to be derived from the relationship of the edge and the angle of the tetrahedron O,I,III,IV. However, if $\theta = \beta = 90°$, ψ cannot be assessed.

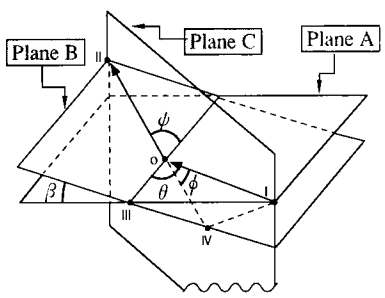

FIGURE 4 Illustration accounting for angle of incidence ϕ, jumping angle ψ, deflecting angle θ, and slope gradient β.

Because the angle of incidence (ϕ) is a key factor governing the velocity reduction coefficient, it can now be understood that to estimate the value of k, it is necessary to perform an experiment in which the angle of incidence is varied. The simplest method for performing a striking experiment in which the angle of incidence is varied is shown in Figure 4: $\theta = \beta = 90°$, and Surface A is horizontal, where $\beta = \phi$ is established simultaneously. This permits the jumping height of an avalanche to be represented as follows from a model of a body that moves on a plane under the effects of bottom surface friction and the resistance of gravity. However, μ is the kinematics friction coefficient of the deflector surface and the snow avalanche.

$$H = \frac{(kV_b)^2 \sin\phi}{2g(\sin\phi + \mu\cos\phi)} \tag{3}$$

Experimental Assessment of Velocity Reduction Coefficient

A horizontal flow of a collection of small snow ice particles was caused to strike a plane, $\theta = 90°$, at varying angles of incidence (ϕ) to measure the striking velocity (V_b) and the run-up height on the plane. The model avalanches flowed down a chute with a length of 3 m and a width of 40 cm. A horizontal table surface was connected to the chute at its bottom end and the model was installed on a table (Figure 5). The velocity of the avalanche when it collided with the model could be varied from 3 to 6 m/sec by varying the gradient of the chute. The model was made of FRP resin panels with a length of 1 m and a width of 2 m. The collision angle θ of the avalanche and the slope gradient β of the collision surface were varied by changing the incline and direction of the panels of the model. A mesh with sides 5 × 5 cm was drawn on the resin panels to measure the behavior of the avalanche. The samples used for the experiment were ice particles with a central grain size of about 1 mm and accumulation density between 0.4 and 0.5 (g/cm^3) prepared by pulverizing ice in a laboratory at a temperature of –10°C. The avalanche collision velocity was found by installing two beam sensors near the bottom of the chute and calculating the velocity from the time gap between two measured points and the distance between the two points.

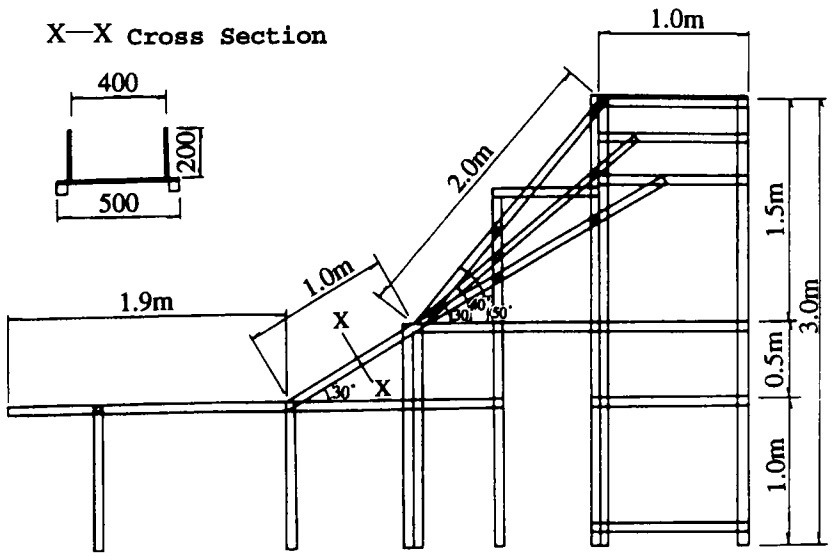

FIGURE 5 Model avalanche chute.

The behavior of a snow avalanche striking a plane varies according to the angle of incidence (ϕ). When ϕ is 45° or 60°, the snow avalanche moves in such a way that it runs up the deflector plane; then, as time passes, the width of the snow avalanche gradually increases. When the angle of incidence is 90°, the snow avalanche not only jumps up along the surface of the deflector when it strikes the surface, but it also sprays to the left and right, forming an expanding semicircle. Part of the tip of the snow avalanche consists of particles that collide with the deflector surface and then bounce back, but this is a temporary condition not repeated by the following snow, and the height at which the snow jumps backward is lower than the height it jumps up. To use Equation 3 to estimate k, it is necessary to set the value of k. Figure 6 is a schematic diagram of the test apparatus used to find the kinematics friction coefficient of the plane and the snow ice particles. As the cart was pulled at a fixed velocity by a motor, the tension of the rope connecting a sampler filled with snow ice particles mounted on top of the cart to the wall was recorded. The recorded data indicate that when the cart was pulled by the motor, breaking the adhesion of the snow ice particles to the deflector surface required large initial force, but that after that stage the force remained almost constant. The experiment was conducted with the sampler filled with snow ice particles and with an empty sampler. When the results for the snow ice particles and for the sampler are represented by the subscripts $_0$ and $_1$ respectively, the results are as follows: from $F_0 = \mu_0 N_0$, $F_1 = \mu_1 N_1$, $F_{0+1} = F_0 + F_1$ to $\mu_0 = (F_{0+1} - F_1)/N_0 = 0.23$. ($F$, μ, and N represent the friction force, kinematics friction coefficient, and vertical effectiveness, respectively.)

Figure 7 shows the relationship of the calculated values obtained by using Equation 3, ignoring k, with the measured snow avalanche jumping height values, revealing that the value of k is found from the inclination of the regression straight line. Figure 8 shows the results of an organization of the relations of the angles of incidence (ϕ) with the estimated velocity reduction coefficient (k). But ϕ is represented as degree.

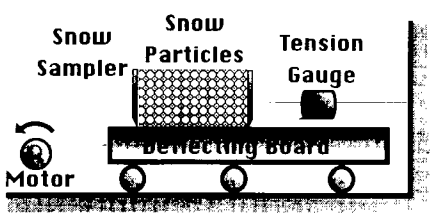

FIGURE 6 Schematic illustration of kinematic friction test.

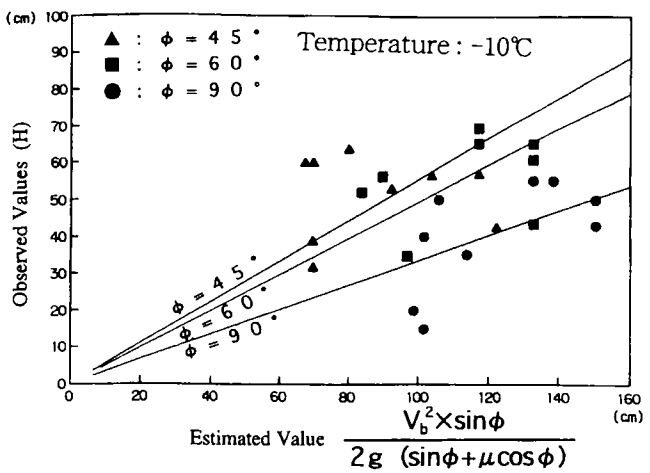

FIGURE 7 Comparison of measured jumping height values and calculated jumping height values.

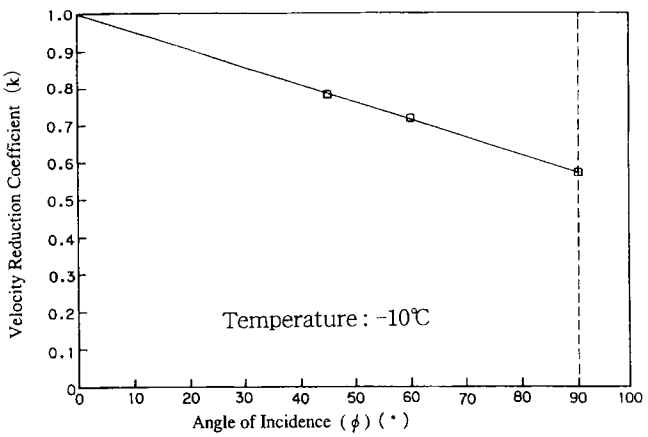

FIGURE 8 Relationship between velocity reduction coefficient and angle of incidence.

$$k = 1 - 4.7 \times 10^{-3} \cdot \phi \tag{4}$$

Study of Run-Up Angle of an Avalanche Striking a Plane

The organization of all the preceding results should permit a description of the avalanche after striking as the motion of an object with the initial conditions run-up velocity kV_b and run-up angle ψ. But in a case in which $\theta = \beta = 90°$, although it was impossible to assess the run-up angle (ψ) by using a motion model of mass points as explained previously, during the experiment the run-up of the snow avalanche could be observed. This suggests differences between the striking phenomenon of mass points on a plane and a flow of concentrated snow ice particles. It can be assumed that the flow of concentrated snow ice particles not only strikes the plane but also influences the run-up angle of the snow avalanche through the collisions between the particles.

When the experiment was performed with the inclination of the deflector surface (β) held constant at 90° and the deflector angle (θ) varied, as shown in Figure 9, several lines were formed on the surface of the snow ice particles that ran up the deflector surface, indicating the course of the motion. Observation of the run-up angle to the surface of the deflector from the course of the motion of the group of particles with the maximum run-up height revealed that this value is the deflector angle (θ). Figure 9 is a schematic diagram of the behavior of an avalanche striking a deflector in a case in which $\beta = 90°$ and $\theta = 60°$. The avalanche that struck the deflector ran up along the surface of the deflector at various run-up angles and formed a fan-shaped front pointed in the deflector direction. As the top of this front flowed in the deflector direction, it separated from the surface of the deflector and fell to rest in front of the deflector. This behavior was observed not only at the front; it continued throughout the entire flow. This reveals that it is not possible to represent the run-up angle when a flow of concentrated particles strikes a plane as a constant value.

When a flow of concentrated particles such as a snow avalanche strikes a plane, the form of motion usually observed after the impact is the particles spreading in the lateral direction. The lateral expansion of the particles is caused by collisions between the particles, and this influences the run-up velocity and run-up angle of the particles. In the case of particles moving from A toward and striking Plane B at angle of incidence ϕ, as shown in Figure 10, flow direction OB after the impact changes only γ degrees to become motion from O toward C. In Plane ABOD, if ψ is defined as the angle of incidence of Plane AOC at right angles to Plane B, ψ can be written as follows:

$$\Phi = \cos^{-1}(\cos\gamma \cdot \cos\phi) \tag{5}$$

If the angle γ is defined in the counterclockwise direction, the run-up angle and the velocity reduction coefficient are corrected as shown, with reference to Equations 2 and 4:

$$\Psi = \psi + \gamma \tag{6}$$

$$K = 1 - 4.7 \times 10^{-3}\Phi \tag{7}$$

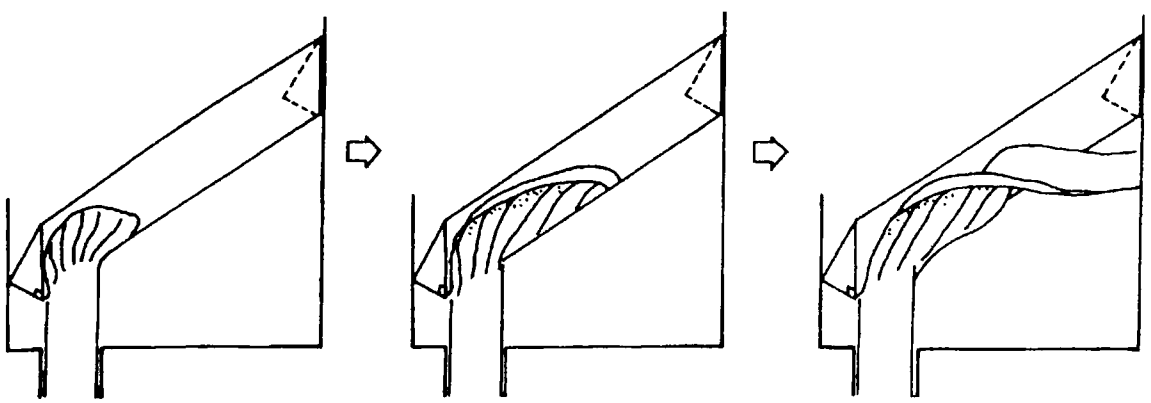

FIGURE 9 Schematic diagram of behavior of snow avalanche striking deflector.

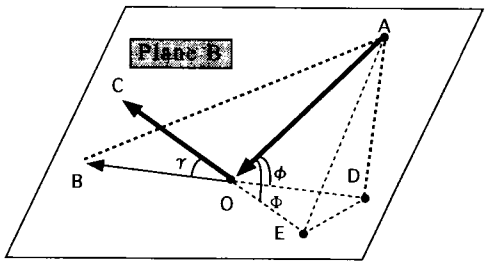

FIGURE 10 Illustration accounting for lateral spread and angles ϕ, Φ, and γ.

Representing the run-up angle and the run-up velocity as the function of the angle γ provides the grounds for the explanation of the behavior (the formation of a fan-shaped front with a tip in the downstream direction as shown in Figure 1 and Figure 9) of a snow avalanche striking a deflector.

The jumping height of the snow avalanche striking Deflector 1 is about 30 m. The height of the action of the friction on the deflector surface is equal to the height of the deflector above the snow, and on the basis of the snow accumulation environment around the deflector as described earlier, the snow depth is estimated to be about 4 m. For these reasons, it is assumed that the jumping height would differ little even if the resistance caused by the friction were ignored. The free motion of an object thrown into the air can be represented as shown in the following and in the coordinate system shown in Figure 11.

$$\frac{dy}{dt} = KV_b \sin\Psi - g\sin\beta \cdot t \tag{8}$$

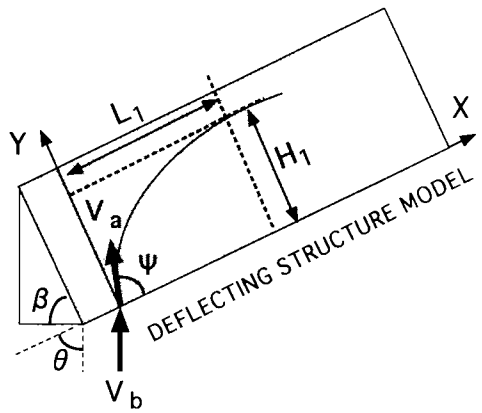

FIGURE 11 Definition of symbols used in analysis.

$$\frac{dx}{dt} = KV_b \cos\Psi \tag{9}$$

Accordingly, H_1 and L_1 are as follows.

$$H_1 = \left(KV_b \sin\Psi\right)^2 / 2g\sin\beta \tag{10}$$

$$L_1 = \left(KV_b\right)^2 \sin\Psi\cos\Psi / g\sin\beta \tag{11}$$

Conditions when the snow avalanche struck Deflector 1 were the following: V_b was 42 m/sec, θ was 45°, β was 84.3°, and the $H_1 - \gamma$ relationship was as shown in Figure 12. The calculated value of γ, which provides the highest value of H_1, is 68°, and $H = H_1 \sin\beta = 35$ m. This result is a little larger than the observed jumping

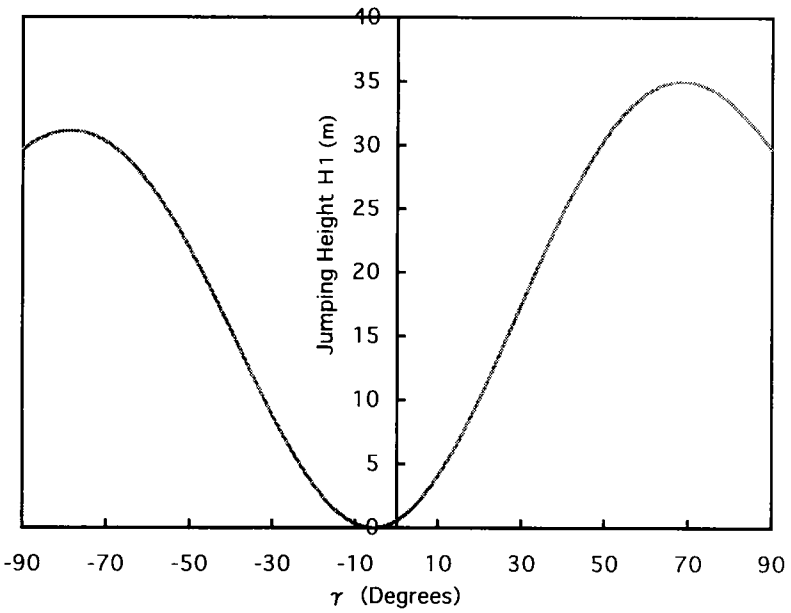

FIGURE 12 Jumping height variations with angle γ.

height of 30 m. The angle at which this avalanche actually ran up the deflector cannot be confirmed because the deflector itself hid the motion, and because only one videotape frame was obtained every 4 sec. Also, the value of L_1 was calculated as 21 m, which is smaller than the jumping length shown in Table 1 (L is 38 m to 77 m). Because the interval between video images was 4 sec, it was impossible to specify the location indicating the maximum jumping height, and because the width of the snow avalanche that jumped was 10 or greater when it struck Deflector 1, it is impossible to conclude that the calculated jumping length was short. At this stage, it would be difficult to verify any more than this; new data are needed.

Summary and Future Challenges

This paper describes the jumping of snow avalanches incorporating the velocity reduction coefficient based on the velocity reduction mechanism and run-up angle of an avalanche striking a plane. An attempt was made to use a single case study to confirm the height and length of the jumping of an avalanche, but because the results were incomplete, more research is necessary.

When a design intended to deal with a high-speed avalanche is planned, it will be difficult to consider realistically a deflector that can handle the jumping height of the avalanche, and the height of the deflector designed will be too small. Accordingly, the shape and height of the deflector surface and its deflector effects must be confirmed. Because it is impossible to ignore the effects of the deposited snow, such as snow blown against the deflector on the effective height of the deflector surface (height above the snow), research on a transparent deflector surface should be performed.

Acknowledgment

The author thanks the Erosion Control Section of the Niigata Prefecture for providing the videotape used for this project.

Reference

1. Kitahara, I., H. Yoshimatsu, and K. Fujisawa. Study of the Mechanics of Debris Flow and Its Simulation Model. *Landslide—Journal of Japan Landslide Society*, Vol. 28, No. 2, Sept. 1991, pp. 9–19.